Finite Control Set Model Predictive Control for Polysolenoid Linear Motor

Nguyen Hong Quang[1], Nguyen Phung Quang[2], Dang Danh Hoang[3,*]
[1,3]Thai Nguyen University of Technology, Viet Nam
[2]Hanoi University of Science and Technology, Viet Nam
[*] *Corresponding author*

Article History: Received: 5 April 2021; Accepted: 14 May 2021; Published online: 22 June 2021

Abstract: In this study, the discontinuity of the voltage source inverter is considered when controlling Polysolenoid motors using model predictive control. When considering the instantaneous voltage across the motor with a non-ideal converter, the set of control voltages is finite and depends on the converter configuration. This is based on the finite control set model predictive controller (FCS MPC). When a finite set of voltage vectors is determined for the stator, the control signal processing capability of the system is significantly improved. Simulations are performed to illustrate the responsiveness of the force loop using the FCS-MPC method.

Key words: MPC, FCS-MPC, Linear Motor, Polysolenoid Linear Motor, FOC.

1. Introduction

The rectilinear motion, which uses a linear motor, can durable operates and achieves higher efficiency than the indirect linear motion. Linear motors are developed based on the working principle of rotating electric machines. The outputs of a linear motor are position and thrust. Linear motors produce displacement and thrust. However, the working principle is classified into many types based on physical properties, such as linear asynchronous motor [1-5], linear synchronous motor [6-11], etc. Polysolenoid linear motor is a permanently excited synchronous motor with a tubular structure. The working principle of Polysolenoid linear motors can be found in [12-21]. Researches on linear motor control are mentioned in many documents [22-29]. The sliding control method is implemented in [22-24]. In [22], an enhanced sliding control structure improves the system accuracy in the high-speed region. The advantages of this method are that the system is stable quickly, and the control structure is simple. A sliding controller combined with an input noise observer is implemented for the outer loop structure [23]. An adaptive-gain sliding mode observer is used in [24] in position control without using a sensor. The Lyapunov stability theory proves the stability of the sliding mode observer (SMO). A fuzzy PID controller, implemented to improve the response of traditional PID for PLMSM, is proposed in [25]. In [26], the extended state observer observes noises and dynamic disturbances of the system. Then, the predictive function controller (PFC) controls the motor speed. An iterative learning control to improve the positioning accuracy of a permanently excited linear motor in the high-speed region is implemented in [27]. The compensation algorithm consists of a PID component and an adaptive component for estimating friction. The adaptive component is continuously refined on the basis of just prevailing input and output signals [28]. In [29], a 4-layer neural network structure to improve position accuracy is implemented. In the above studies, we see that the influence of the motor power supply on the dynamic response of the system has not been properly considered. In this study, the discontinuity of the voltage source inverter due to the nature of the electronic components is analyzed in detail for its ability to generate thrust response for the Polysolenoid motor. Next, the predictive control method with discontinuity of the converter is implemented to evaluate the responsiveness of the force loop.

2. MPC Preliminaries

Model predictive control (MPC), started in the late 70s, has made significant progress. The concept of "model predictive control" not only specifies a specific control strategy but also provides a class of control methods based on using the model of the control object to obtain a minimum cost function. The relationship between the traditional optimal control and the MPC is to use the concept of the cost function to form the control strategy. The concept of "predictive" here is the estimation of the system behavior in the future (predictive range) through which a suitable control signal can be given. Different from the traditional optimal control, the optimal solution of MPC is established based on solving given optimization problems. Therefore, it is challenging to react to uncertain system changes such as noise, model error, etc. The optimal control signal based on MPC is a series of control signals in which each element sequence represents a control signal at a specific k^{th} time. The optimization problem is repeated at every cycle with the latest information about the system. Fig. 1 shows the basic configuration of the model predictive control system.

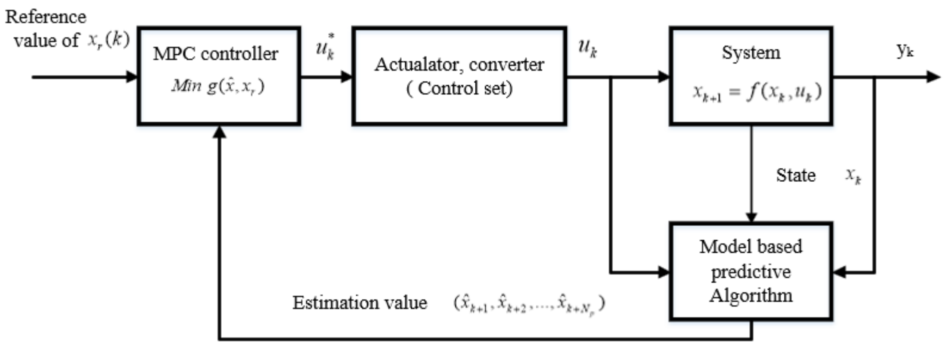

Figure 1: Structure Diagram of MPC.

To illustrate the MPC control structure, we consider a discontinuous system $x_{k+1} = f(x_k, u_k), y_k = h(x_k)$ with u_k is control input, y_k is output, and x_k is state variable. The model oriented predictor provides estimated states, $\hat{x}_{k+1} = f_k(x_k, u_k)$,…, $\hat{x}_{k+N_p} = f_{k+i}(\hat{x}_{k+N_p-1}, u_{k+i})$, which are inputs to the MPC-based optimal controller. The control signal is defined directly by solving the optimal problem $\underset{u_k, u_{k+1}, ..., u_{k+N_c}}{\text{Min}} g(\hat{x}, x_r)$, in which the predictive ranges N_p and N_c are two basic parameters of MPC directly determining the computational value of the controller, $g(\hat{x}, x_r)$ is cost function of the reference value x_r, and $\hat{x} = [\hat{x}_{k+1}, ..., \hat{x}_{k+N_p}]$ is the estimated value.

3. Design of FCS-MPC for the Current Loop

The Polysolenoid motor considered in this study belongs to the group of permanently excited synchronous linear motors with a short stator structure. The structure of the motor is shown in Figure 2.

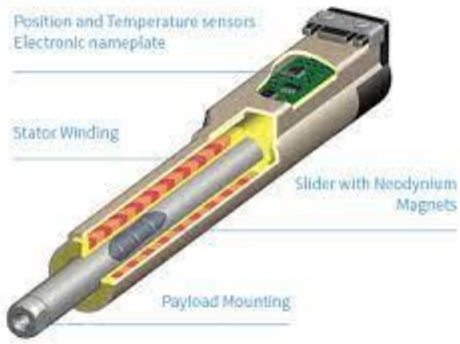

Figure 2: Polyslenoidlinear Motor [13].

The mathematical model of Polysolenoid engine on the dq-coordinate system is given as below [21]:

$$\begin{cases} \dfrac{di_{sd}}{dt} = -\dfrac{R_s}{L_{sd}} i_{sd} + \left(\dfrac{2\pi p}{\tau} v\right) \dfrac{L_{sq}}{L_{sd}} i_{sq} + \dfrac{u_{sd}}{L_{sd}} \\ \dfrac{di_{sq}}{dt} = -\dfrac{R_s}{L_{sq}} i_{sq} - \left(\dfrac{2\pi}{\tau} v\right) \dfrac{L_{sd}}{L_{sq}} i_{sd} - \left(\dfrac{2\pi p}{p\tau} v\right) \dfrac{\psi_p}{L_{sq}} + \dfrac{u_{sq}}{L_{sq}} \\ \dfrac{dv}{dt} = \dfrac{2\pi p}{\tau} \left(\psi_p + (L_{sd} - L_{sq}) i_{sd}\right) i_{sq} - \dfrac{1}{m} F_c \\ \dfrac{dx}{dt} = v \end{cases} \tag{1}$$

From (1), we derive the continuous current model of the Polysolenoid motor on the dq-coordinate system as

$$\frac{d\mathbf{i}_{dq}}{dt} = \mathbf{A}\mathbf{i}_{dq} + \mathbf{B}\mathbf{u}_{dq} + \mathbf{N}\mathbf{i}_{dq}\omega_e + \mathbf{S}\psi_p\omega_e \tag{2}$$

Where

$$\mathbf{i}_{dq}{}^T = \begin{bmatrix} i_d & i_q \end{bmatrix}, \mathbf{u}_{dq}{}^T = \begin{bmatrix} u_d & u_q \end{bmatrix}$$

$$\mathbf{A} = \begin{bmatrix} -\frac{R_s}{L_d} & 0 \\ 0 & -\frac{R_s}{L_q} \end{bmatrix},\ \mathbf{B} = \begin{bmatrix} \frac{1}{L_d} & 0 \\ 0 & \frac{1}{L_q} \end{bmatrix},\ \mathbf{N} = \begin{bmatrix} 0 & \frac{L_q}{L_d} \\ -\frac{L_d}{L_q} & 0 \end{bmatrix},\ \mathbf{S} = \begin{bmatrix} 0 \\ -\frac{1}{L_q} \end{bmatrix}.$$

The discrete-time stator current model of Polysolenoid motor is:

$$\mathbf{i}_{dq}(k+1) = \mathbf{\Phi}\mathbf{i}_{dq}(k) + \mathbf{H}\mathbf{u}_{dq}(k) + \mathbf{h}\psi_p \tag{3}$$

From the above discrete-time model, we build a predictive model with $\mathbf{i}_{dq}^{est}(k+i)$ is the predicted current value at the next i-th cycle compared to the current time. From the (3), we have:

$$\mathbf{i}_{dq}^{est}(k+i+1|k) = \mathbf{\Phi}\mathbf{i}_{dq}^{est}(k+i|k) + \mathbf{H}\bar{\mathbf{u}}_{dq}(k+i) + \mathbf{h}\psi_p \tag{4}$$

The selected objective function has the following quadratic form:

$$J = \sum_{i=1}^{N_p}\left[\left(\mathbf{i}_{dq}^{ref} - \mathbf{i}_{dq}^{est}(k+i\,|\,k)\right)^T \mathbf{Q}\left(\mathbf{i}_{dq}^{ref} - \mathbf{i}_{dq}^{est}(k+i\,|\,k)\right)\right] \tag{5}$$

Where N_p is the prediction range.

Solving the optimization problem by the FCS-MPC method can be done quickly with a finite number of loops. However, the number of iterations will increase exponentially in the prediction range, which leads to a significant increase in computation time and loss of the advantage of the method. Therefore, in this case, we choose the prediction range as $N_p = 2$.

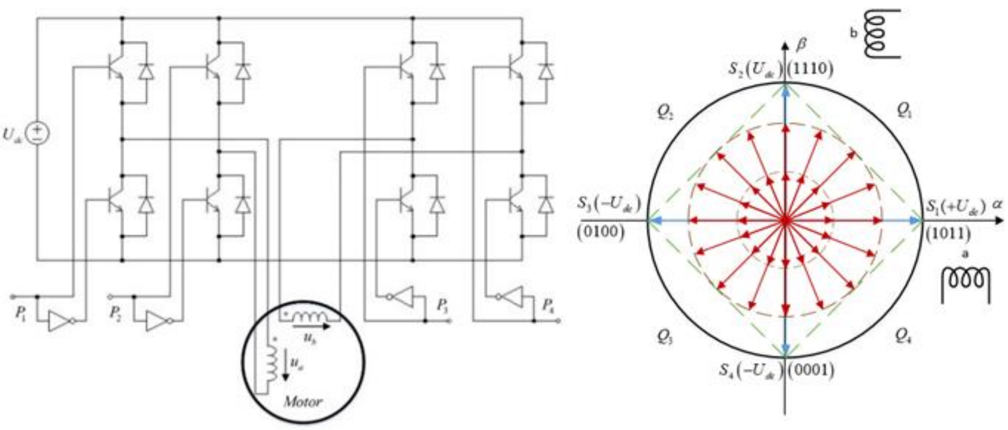

Figure 3: Distribution of the Basis Vectors of the Inverter Circuit According to FCS-MPC.

The optimization problem is now reduced to the form:

$$\begin{aligned} \min_{\bar{\mathbf{u}}_{dq}(k),\bar{\mathbf{u}}_{dq}(k+1)} J = {} & \bar{\mathbf{u}}_{dq}(k)^T\left(\mathbf{H}^T\mathbf{Q}\mathbf{H}\right)\bar{\mathbf{u}}_{dq}(k) + \bar{\mathbf{u}}_{dq}(k+1)^T\left(\mathbf{H}^T\mathbf{Q}\mathbf{H}\right)\bar{\mathbf{u}}_{dq}(k+1) \\ & + \bar{\mathbf{u}}_{dq}(k)^T\left(\mathbf{H}^T\mathbf{Q}^T\mathbf{Q}\mathbf{H}\right)\bar{\mathbf{u}}_{dq}(k+1) \\ & + 2\left(\mathbf{\Phi}\mathbf{i}_{dq}(k) + \mathbf{h}\psi_p - \mathbf{i}_{dq}^{ref}\right)^T \mathbf{Q}\mathbf{H}\bar{\mathbf{u}}_{dq}(k) \\ & + 2\left(\mathbf{\Phi}^2\mathbf{i}_{dq}(k) + \mathbf{\Phi}\mathbf{h}\psi_p - \mathbf{i}_{dq}^{ref}\right)^T \mathbf{Q}\mathbf{H}\bar{\mathbf{u}}_{dq}(k+1) \end{aligned} \tag{6}$$

Satisfy: $\bar{\mathbf{u}}_{dq} \in \mathbf{U} \triangleq \left\{\mathbf{R}\mathbf{u}_{S_1}, \mathbf{R}\mathbf{u}_{S_2}, \mathbf{R}\mathbf{u}_{S_3}, \mathbf{R}\mathbf{u}_{S_4}, \ldots, \mathbf{R}\mathbf{u}_{Sn}, \mathbf{u}_0\right\}$

Where $\mathbf{u}_{S_i}$ is the stator voltage vector generated by the switching state S_i, as illustrated in Figure 3, $\mathbf{u}_0$ is the zero sequence voltage vector, $\mathbf{i}_{dq}^{ref}$ is the reference current vector.

4. Simulation Result

Motor parameters are described in Table. 1.

Table 1: Motor Parameters

Motor Parameters	Symbol	Value	Unit
d-axis stator inductance	L_{sd}	1.4	mH
q-axis stator inductance	L_{sq}	1.4	mH
Stator resistance	R_s	10.3	Ω
Rotor flux	ψ_p	0.035	Wb
Number of pole pairs	z_p	2	
Pole step	τ_p	0.02	m

Simulation is performed with the current sampling time $T_i = 100(\mu s)$. Responses of the FCS-MPC current regulator to a change in the current loop reference value as shown in Fig. 4 and Fig. 5.

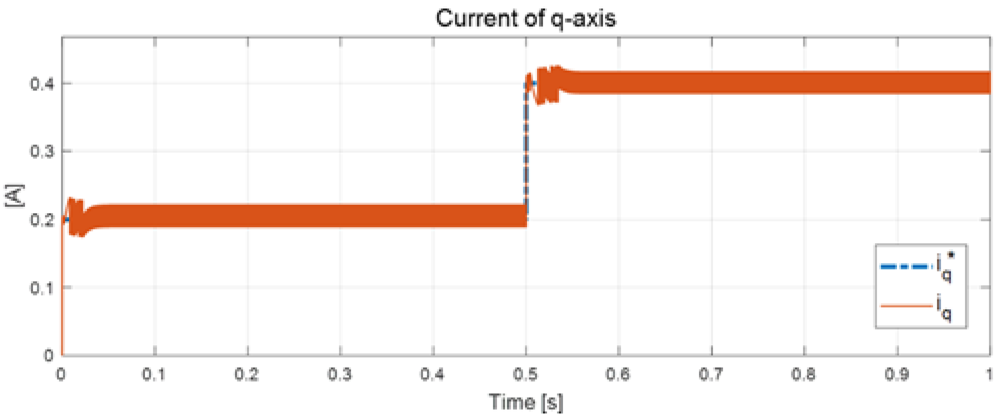

Figure 4: i_qCurrent Response.

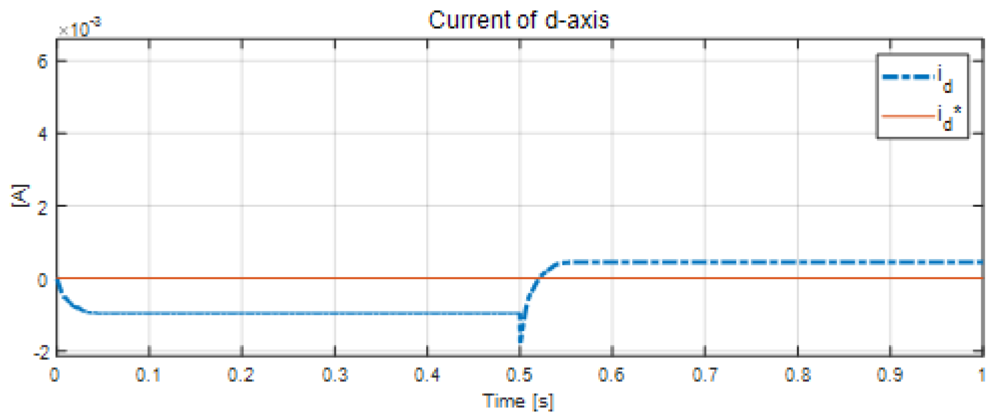

Figure 5: i_dCurrent Response.

Comment: At the time of changing the q-axis current value, the q-axis current value tracks the reference value, as shown in Figure 4. The d-axis current value is also returned to a value close to 0. The tracking error of d-axis current value is insignificant, as depicted in Figure 5. The current pattern of the FCS-MPC method has a non-smooth form and has an unnoticeable amount of overshoot. The response current value still adheres to the reference value precisely, indicating the selected number of base vectors meets the requirements. To improve the current smoothness, we can increase the number of base vectors.

5. Conclusions

When applying the FCS-MPC control method for Polysolenoid motors, we find that with discontinuous objects such as power converters, the FCS-MPC is an effective method. It offers a completely different approach to power converters. Besides, the technical characteristics of the controller also proved to be very good compared with existing control methods. This method is based on a finite number of possible valve combinations of the power converter. Similar to other MPC controllers, FCS- MPC also needs an objective function J so that suitable valve combinations can be selected. The advantage of FCS-MPC over classical MPC methods is that the optimal solution is always guaranteed to have a solution, and the number of computations is significantly reduced.

Acknowledgments

This research was funded by Thai Nguyen University of Technology, No. 666, 3/2 street, Thai Nguyen, Viet Nam.

References

1. Higuchi, T., Nonaka, S., & Ando, M. (2001). On the design of high-efficiency linear induction motors for linear metro. Electrical Engineering in Japan, 137(2), 36-43.
2. Abdollahi, S. E., Mirzayee, M., & Mirsalim, M. (2015). Design and analysis of a double-sided linear induction motor for transportation. IEEE Transactions on magnetics, 51(7), 1-7.
3. Gastli, A. (1998). Conductors of a linear induction motor. IEEE transactions on Energy Conversion, 13(2), 111-116.
4. Johnson, A. P. (2005). High speed linear induction motor efficiency optimization. MASSACHUSETTS INST OF TECH CAMBRIDGE.
5. Hall, D., Kapinski, J., Krefta, M., & Christianson, O. (2008). Transient electromechanical modeling for short secondary linear induction machines. IEEE Transactions on Energy Conversion, 23(3), 789-795.
6. Ferkova, Z., Franko, M., Kuchta, J., & Rafajdus, P. (2008, June). Electromagnetic design of ironless permanent magnet synchronous linear motor. In 2008 International Symposium on Power Electronics, Electrical Drives, Automation and Motion (pp. 721-726). IEEE.
7. Yao, Z., Zhao, J., Song, J., Dong, F., He, Z., & Zong, K. (2020). Research on Selection Criterion of Design Tolerance for Air-Core Permanent Magnet Synchronous Linear Motor. IEEE Transactions on Industrial Electronics, 68(4), 3336-3347.
8. Lim, K. C., Woo, J. K., Kang, G. H., Hong, J. P., & Kim, G. T. (2002). Detent force minimization techniques in permanent magnet linear synchronous motors. IEEE Transactions on Magnetics, 38(2), 1157-1160.
9. Jiefan, C., Chengyuan, W., Junyou, Y., & Dongbo, Y. (2004, November). Research on force and direct thrust control for a permanent magnet synchronous linear motor. In 30th Annual Conference of IEEE Industrial Electronics Society, 2004. IECON 2004 (Vol. 3, pp. 2269-2272). IEEE.
10. Xing, F., Kou, B., Zhang, L., Wang, T., & Zhang, C. (2018). Analysis and Design of a Maglev Permanent Magnet Synchronous Linear Motor to Reduce Additional Torque in dq Current Control. Energies, 11(3), 556.
11. Li, L., Xuzhen, H., Donghua, P., & Jiwei, C. (2010). Magnetic field of a tubular linear motor with special permanent magnet. IEEE Transactions on Plasma Science, 39(1), 83-86.
12. Ausderau, D. (2004). Polysolenoid-Linearantrieb mit genutetem Stator (Doctoral dissertation, ETH Zurich).
13. LinMot Company Home Page: Products, Linear Motors. Available online: https://linmot.com/products/linear-motors/ (accessed on 1 March 2020).
14. Nguyen, Q. H., Dao, N. P., Nguyen, T. T., Nguyen, H. M., Nguyen, H. N., & Vu, T. D. (2016). Flatness based control structure for polysolenoid permanent stimulation linear motors. SSRG International Journal of Electrical and Electronics Engineering, 3(12), 31-37.
15. Quang, N. H. (2017). Multi parametric programming based model predictive control for tracking control of polysolenoid linear motor. Special issue on Measurement, Control and Automation, 19, 31-37.
16. Quang, N. H., Quang, N. P., & Hien, N. N. (2020). On tracking control problem for polysolenoid motor model predictive approach. International Journal of Electrical & Computer Engineering (2088-8708), 10(1).
17. Nguyen, H. Q. (2020, March). Observer-Based Tracking Control for Polysolenoid Linear Motor with Unknown Disturbance Load. In Actuators (Vol. 9, No. 1, p. 23).
18. Nam, D. P., Quang, N. H., Hung, N. M., & Ty, N. T. (2017, July). Multi parametric programming and exact linearization based model predictive control of a permanent magnet linear synchronous motor. In 2017 International Conference on System Science and Engineering (ICSSE) (pp. 743-747). IEEE.
19. Ty, N. T., Hung, N. M., Nam, D. P., & Quang, N. H. (2018). A Laguerre model-based model predictive control law for permanent magnet linear synchronous motor. In Information Systems Design and Intelligent Applications (pp. 304-313). Springer, Singapore.

20. Quang, N. H., Quang, N. P., Nam, D. P., & Binh, N. T. (2019). Multi parametric model predictive control based on laguerre model for permanent magnet linear synchronous motors. International Journal of Electrical and Computer Engineering (IJECE), 9(2), 1067-1077.
21. Nguyen, H. Q., Nguyen, P. Q., Nguyen, N. H., & Nguyen, T. B. (2018). Min max model predictive control for polysolenoid linear motor. International Journal of Power Electronics and Drive Systems, 9(4), 1666.
22. Jiang, D., Yu, W., Wang, J., Zhao, Y., Li, Y., & Lu, Y. (2019). A speed disturbance control method based on sliding mode control of permanent magnet synchronous linear motor. IEEE Access, 7, 82424-82433.
23. Aschemann, H., Haus, B., & Mercorelli, P. (2018, June). Sliding mode control and observer-based disturbance compensation for a permanent magnet linear motor. In 2018 Annual American Control Conference (ACC) (pp. 4141-4146). IEEE.
24. Yang, C., Ma, T., Che, Z., & Zhou, L. (2017). An adaptive-gain sliding mode observer for sensorless control of permanent magnet linear synchronous motors. IEEE Access, 6, 3469-3478.
25. Hua, S., & Dai, Y. (2010, June). Fuzzy PID control and simulation experiment on permanent magnet linear synchronous motors. In 2010 International Conference on Electrical and Control Engineering (pp. 1047-1049). IEEE.
26. Wang, Y., Yu, H., Che, Z., Wang, Y., & Zeng, C. (2019). Extended state observer-based predictive speed control for permanent magnet linear synchronous motor. Processes, 7(9), 618.
27. Hama, T., & Sato, K. (2015). High-speed and high-precision tracking control of ultrahigh-acceleration moving-permanent-magnet linear synchronous motor. Precision engineering, 40, 151-159.
28. Tan, K. K., Huang, S. N., & Lee, T. H. (2002). Robust adaptive numerical compensation for friction and force ripple in permanent-magnet linear motors. IEEE Transactions on Magnetics, 38(1), 221-228.
29. Cailin, L., & Dongmei, W. (2013, September). The permanent magnet synchronous linear motor position control based on fuzzy neural network. In 2013 5th International Conference on Intelligent Networking and Collaborative Systems (pp. 602-606). IEEE